Effect of Nuclear Factor κB Inhibition on Serotype 9 Adeno-Associated Viral (AAV9) Minidystrophin Gene Transfer to the *mdx* Mouse

Daniel P Reay,[1,2] Gabriela A Niizawa,[1,2] Jon F Watchko,[3] Molly Daood,[3] Ja'Nean C Reay,[2,4] Eugene Raggi,[2] and Paula R Clemens[1,2]

[1]Neurology Service, Department of Veterans Affairs Medical Center, Pittsburgh, Pennsylvania, United States of America; [2]Department of Neurology, University of Pittsburgh, Pittsburgh, Pennsylvania, United States of America; [3]Department of Pediatrics, Magee-Women's Research Institute, University of Pittsburgh, Pittsburgh, Pennsylvania, United States of America; and [4]Lake Erie College of Osteopathic Medicine (LECOM) at Seton Hill University, Greensburg, Pennsylvania, United States of America

Gene therapy studies for Duchenne muscular dystrophy (DMD) have focused on viral vector-mediated gene transfer to provide therapeutic protein expression or treatment with drugs to limit dystrophic changes in muscle. The pathological activation of the nuclear factor (NF)-κB signaling pathway has emerged as an important cause of dystrophic muscle changes in muscular dystrophy. Furthermore, activation of NF-κB may inhibit gene transfer by promoting inflammation in response to the transgene or vector. Therefore, we hypothesized that inhibition of pathological NF-κB activation in muscle would complement the therapeutic benefits of dystrophin gene transfer in the *mdx* mouse model of DMD. Systemic gene transfer using serotype 9 adeno-associated viral (AAV9) vectors is promising for treatment of preclinical models of DMD because of vector tropism to cardiac and skeletal muscle. In quadriceps of C57BL/10ScSn-*Dmd^mdx*/J (*mdx*) mice, the addition of octalysine (8K)–NF-κB essential modulator (NEMO)-binding domain (8K-NBD) peptide treatment to AAV9 minidystrophin gene delivery resulted in increased levels of recombinant dystrophin expression suggesting that 8K-NBD treatment promoted an environment in muscle tissue conducive to higher levels of expression. Indices of necrosis and regeneration were diminished with AAV9 gene delivery alone and to a greater degree with the addition of 8K-NBD treatment. In diaphragm muscle, high-level transgene expression was achieved with AAV9 minidystoophin gene delivery alone; therefore, improvements in histological and physiological indices were comparable in the two treatment groups. The data support benefit from 8K-NBD treatment to complement gene transfer therapy for DMD in muscle tissue that receives incomplete levels of transduction by gene transfer, which may be highly significant for clinical applications of muscle gene delivery.
Online address: http://www.molmed.org
doi: 10.2119/molmed.2011.00404

INTRODUCTION

Duchenne muscular dystrophy (DMD) is an X-linked genetic disorder caused by a mutation in the *DMD* gene and is the most common muscular dystrophy, occurring in about 1 in every 3,500 live male births (1). It is characterized by progressive wasting of skeletal and cardiac muscles, resulting in loss of ambulation by the teenage years and death due to cardiac or respiratory failure by the third decade (2). Current treatments can delay deterioration of muscle function but do not halt the disease process. Use of gene therapy to replace the dysfunctional dystrophin gene is promising; however, delivery to widespread muscles has proved to be a significant challenge.

Dystrophin, a 427-kDa protein, plays a vital structural role linking the internal cytoskeleton to the extracellular matrix through the dystrophin-associated protein complex (DAPC) and provides sarcolemmal localization to other proteins important in muscle health (3–5). In human DMD as well as in the murine disease model of DMD, the C57BL/10ScSn-*Dmd^mdx*/J (*mdx*) mouse, loss of sarcolemmal localized dystrophin protein not only leads to loss of the DAPC, but also triggers a cascade of events leading to a persistent inflammatory response, degeneration of both skeletal and cardiac muscle and replacement of muscle tissue with adipose and connective tissues (2,3,6). DMD is a single-gene disorder, making it an attractive candidate for

gene replacement therapy, which has been studied extensively in dystrophin-deficient animal models. One of the more promising vector systems for muscle gene transfer is on the basis of the adeno-associated virus (AAV). Although the AAV vector has a limited transgene-carrying capacity, internally deleted, truncated minidystrophin cDNA transgenes can be delivered by the AAV vector. These vectors have demonstrated high levels of transgene expression, localization of recombinant dystrophin to the sarcolemmal membrane, restoration of the DAPC, amelioration of dystrophic histopathology and functional improvement in hindlimb and diaphragm skeletal muscle (7,8). Among the different AAV serotypes, AAV serotype 9 (AAV9) vectors efficiently transduce skeletal and cardiac muscle after a systemic administration (9,10).

Despite efficient gene transduction by AAV9 vectors, some disease pathology persists because of incomplete rescue of the dystrophic phenotype and possible immune responses to either the vector or recombinant dystrophin (11,12). Recent studies have begun to elucidate upregulated intracellular pathways responsible for the inflammatory response in the *mdx* mouse. Nuclear factor (NF)-κB, a mammalian transcription factor, shows high levels of activation in dystrophic tissues (13–19). Although there are a wide range of processes that NF-κB can mediate, the inflammatory response and inhibition of muscle regeneration are among the primary roles of NF-κB in dystrophic tissue (13). The NF-κB family consists of five subunits: RelA/p65, RelB, c-Rel, p105/52 and p100/50; functional NF-κB proteins are composed of subunit dimers that are sequestered in the cytoplasm by the inhibitor protein IκB (20). Previous studies in mice bred a heterozygous deletion of the NF-κB-p65 subunit crossed onto the *mdx* genetic background. These *mdx* mice that were deficient in p65 expression demonstrated diminished NF-κB activation and improved dystrophic histopathology compared to *mdx* mice with normal levels of p65 (13).

Furthermore, administration of a NF-κB essential modulator (NEMO)-binding domain (NBD) peptide that contains a sequence of amino acids complementary to the IκB kinase γ (IKKγ)-binding domain for the catalytic IKKβ subunit of the IKK complex inhibits NF-κB activation and has demonstrated beneficial therapeutic effects in *mdx* mice (18,21). Systemic delivery of the NBD peptide was achieved by using a fusion peptide, linking the NBD peptide to the protein transduction domain (PTD) octalysine (8K), from a class of cationic, cell-penetrating peptides that can effectively transport therapeutic peptides intracellularly (22).

We therefore tested the hypothesis that inhibition of NF-κB by administration of the NBD peptide would enhance the therapeutic benefit provided by AAV9 minidystrophin gene transfer to *mdx* mice.

MATERIALS AND METHODS

AAV Vector and 8K-NBD Peptide Production

The AAV9 δ3978 cytomegalovirus (CMV)-opti-dys minidystrophin vector (referred to hereafter as AAV9 minidystrophin vector) was produced as previously described (7,23). The expression cassette in the AAV9 minidystrophin vector is a codon-optimized, human minidystrophin cDNA driven by the CMV promoter. The purified AAV9 minidystrophin vector stock had a titer of 8.8×10^{12} vector genomes (vg)/mL determined by dot-blot assay. 8K-NBD peptide was synthesized at the Peptide Synthesis Facility (University of Pittsburgh, Pittsburgh, PA, USA). The 8K PTD was linked to the therapeutic NBD peptide by a two-glycine spacer element. Therefore, the fusion peptide amino acid sequence was KKKKK KKKGG TALDA SALQT E (18). Lyophilized 8K-NBD peptide was resuspended in sterile, deionized water to a 40 mmol/L concentration, and biological activity was confirmed by reducing tumor necrosis factor (TNF)-α–induced NF-κB activation in C2C12 cells *in vitro*.

Mice and Administration of AAV Vector and PTD-NBD Peptides

C57BL/10 and C57BL/10ScSn-*Dmd^mdx*/J mice were purchased from The Jackson Laboratory (Bar Harbor, ME, USA) and housed in the Biomedical Science Tower Animal Facility at the University of Pittsburgh. Mouse rooms were equipped with light-, humidity- and temperature-controlled environments, and mice were provided food and water *ad libitum*. Two-day-old neonatal *mdx* mice received an intraperitoneal injection of 1×10^{11} vg/mouse of AAV9 minidystrophin vector. Administration of 10 mg/kg 8K-NBD peptide or saline by intraperitoneal injection three times per week began at 28 d of age and continued for 5 wks. Age-matched, untreated C57BL/10 mice provided a healthy control group, whereas age-matched, untreated *mdx* mice represented the dystrophic control group. Muscles, organs and serum were harvested after sacrifice by thoracic disruption during *ex vivo* functional analysis of the diaphragm muscle. All studies were approved by the University of Pittsburgh Institutional Animal Care and Use Committee.

Mouse Diaphragm Functional Analysis

After the final 8K-NBD peptide or saline administration at 9 wks of age, experimental and control mice were anesthetized with 50 mg/kg pentobarbital and regions of costal diaphragm muscle, with one end connected to the ribcage, were excised. Isolated costal diaphragm muscles were first analyzed for specific force (N/cm^2) and then subjected to 10 lengthening activations to analyze isometric force generation in response to physiological stress. Diaphragmatic physiological muscle function procedures were previously described (8,24).

Immunohistochemistry and Hematoxylin and Eosin Staining

Cryosections (10 μm) from quadriceps, gastrocnemius, tibialis anterior, triceps, tongue, heart and costal diaphragm were immunostained to assess levels of minidystrophin expression by first blocking

endogenous mouse IgG with the M.O.M. blocking reagent (Vector Labs, Burlingame, CA, USA). Sections were incubated with a 1:20 dilution of dystrophin antibody corresponding to the N-terminus, clone Dy10/12B2 (Vector Labs), followed by 1:250 diluted Alexa Fluor® 488–conjugated goat anti-mouse IgG secondary antibody (Invitrogen, Carlsbad, CA, USA). Nuclear staining was achieved using 4′,6-diamidino-2-phenylindole (DAPI)-fluoromount G mounting media (Southern Biotech, Birmingham, AL, USA). Necrotic muscle fibers were detected by incubation of tissue sections with a 1:100 dilution of Labs), followed by 1:250 diluted Alexa Fluor 488 rabbit anti-mouse IgG antibody (Invitrogen). Levels of regeneration were assessed by incubation of cryosections with a 1:10 diluted embryonic myosin heavy-chain supernatant antibody, F1.652. This antibody was developed by Helen Blau and was obtained from the Developmental Studies Hybridoma Bank, developed under the auspices of the National Institute of Child Health & Human Development (NICHD) and maintained by the University of Iowa, Department of Biological Sciences (Iowa City, IA, USA). This step was followed by 1:250 diluted Labs), followed by 1:250 diluted Alexa Fluor 488–conjugated goat anti-mouse IgG (Invitrogen). Levels of necrosis and regeneration were determined by counting positive muscle fibers in two complete and independent sections obtained from regions separated by a minimum of 300 μm near the midsection of each muscle. The data were expressed as the average percent positive muscle fibers per whole section. Hematoxylin and eosin (Sigma, St. Louis, MO, USA) staining was performed on sections according to standard protocols.

Western Blot Analysis

A 25-mg sample of frozen muscle tissue (quadriceps, heart and diaphragm) was lightly pulverized with a mortar and pestle on dry ice. Total protein was extracted using 50 μL of the T-PER Tissue Protein Extraction Reagent (Pierce/

ThermoFisher Scientific, Rockford, IL, USA) with brief homogenization, followed by centrifugation at 10,000g for 5 min. Protein content was determined by BCA Protein Assay (Pierce/Thermo-Fisher Scientific). A total of 50 μg protein was mixed with a volume of 5× Laemmli buffer (62.76 mmol/L Tris-HCl, pH 6.8, 10% glycerol, 1% sodium dodecyl sulfate (SDS), 0.01% bromophenol blue and 1% β-mercaptoethanol), heated at 94°C for 5 min and run on a 7.5% denaturing polyacrylamide gel at 100 V for 90 min. Protein was transferred to nitrocellulose membranes (GE Healthcare, Piscataway, NJ, USA) at 100 V for 1 h, followed by blocking with 1× TBS, 0.1% Tween-20, 5% w/v skim milk and 5% sheep serum. The 169-kDa minidystrophin band was observed after incubating a 1:20 diluted dystrophin antibody, corresponding to the N-terminus, clone Dy10/12B2 (Vector Labs), followed by incubation with a 1:5,000 horseradish peroxidase (HRP)-sheep-anti-mouse IgG secondary antibody (GE Healthcare) and detected using the enhanced chemiluminescence (ECL) reagent (GE Healthcare). Blots were exposed to autoradiographic film for 20 h. Blots were stripped and reprobed for a 38-kDa glyceraldehyde-3-phosphate dehydrogenase (GAPDH) band as a loading control with a 1:500 diluted rabbit anti-GAPDH antibody (Santa Cruz Biotechnology, Santa Cruz, CA, USA) followed by a 1:2,000 diluted HRP-goat-anti-rabbit IgG secondary antibody (Santa Cruz Biotechnology). GAPDH-probed blots were exposed to autoradiographic film for 3 min. All autoradiographic films were scanned, and densitometry was performed using ImageJ software (Wayne Rasband, NIH, Bethesda, MD, USA; http://imagej.nih.gov/ij/index.html). Minidystrophin expression values were normalized to GAPDH loading control values.

**NF-κB Electrophoretic Mobility Shift Assay**

Nuclear protein was extracted from 25 mg quadriceps and diaphragm tissues using the NE-PER Nuclear Extraction Kit,

according to the manufacturer's instructions (Pierce/ThermoFisher Scientific). Tissues were pulverized on dry ice with a mortar and pestle before extraction to ensure proper homogenization of samples. Multiple dilutions of nuclear extract were prepared and assayed for protein content using the BCA Protein Assay Kit to enable equal loading of samples. The double-stranded DNA probe containing the NF-κB consensus–binding domain was radiolabeled using α-^{32}P-deoxycytodine triphosphate as previously described (18). A total of 50 μg nuclear extract was incubated with 5× Gel Shift Buffer (Promega, Madison, WI, USA) in a 9-μL volume followed by incubation with 1-μL radiolabeled probe at 100,000 counts per min/μL for 25 min. Before addition of samples, 6% nondenaturing polyacrylamide gels were prerun at 300 V for 10 min, and once loaded, gels were run at 300 V for 90 min. Gels were transferred to Whatman paper, weighted flat and dried in an 80°C oven for 60 min, followed by exposure to autoradiographic film for 48–72 h at –80°C. Films were scanned and densitometry was performed using ImageJ software.

Quantitative Real-Time Polymerase Chain Reaction for Vector Genome and mRNA Transcript Analysis

Genomic DNA from 25 mg quadriceps tissue was extracted using the AllPrep DNA/RNA/Protein Mini Kit (Qiagen, Valencia, CA, USA) according to the manufacturer's instructions. rAAV9 minidystrophin vector DNA was isolated using the QIAmp DNA Mini Kit (Qiagen). Quantification of vector DNA was determined using the Quant-iT Oligreen ssDNA Reagent Kit (Invitrogen). Genomic DNA samples were analyzed with primers and a dual-hybridization probe specific for (a) a human minidystrophin construct in the AAV9 minidystrophin vector and (b) mouse apolipoprotein B (*ApoB*), a reference gene used to determine the number of myonuclei in each sample. The data are presented as vector genomes/nucleus. Vector mRNA transcripts were extracted from 25 mg
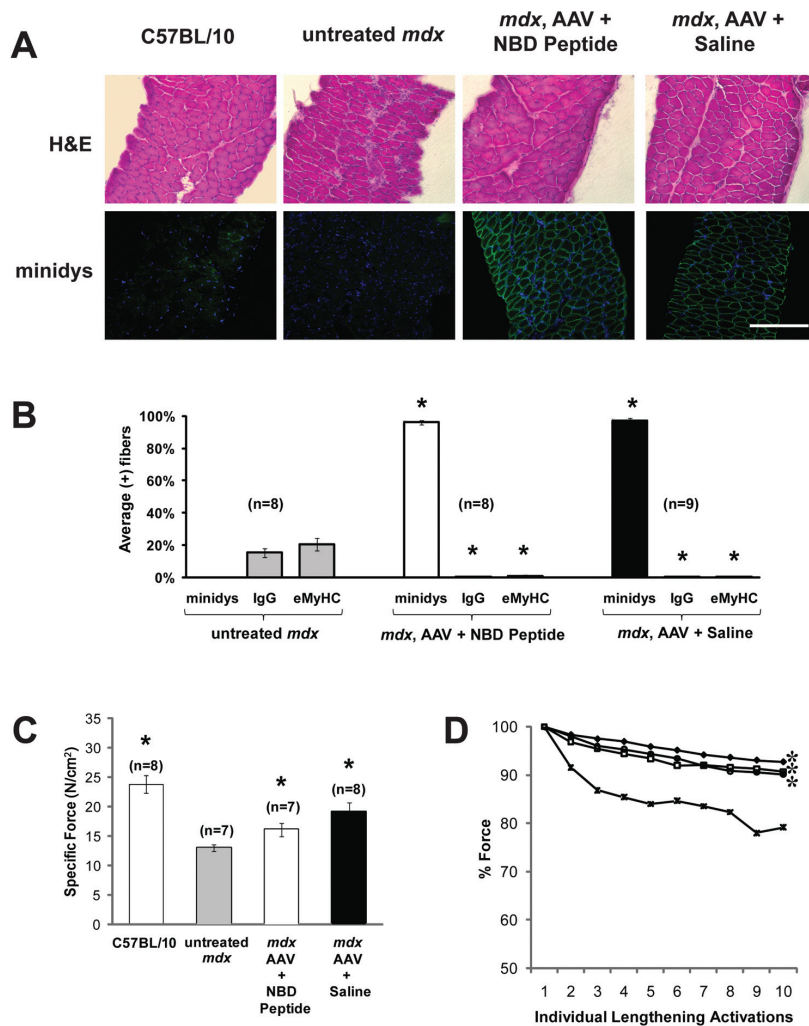
Figure 1. Morphology, human minidystrophin expression and *ex vivo* muscle function analysis of diaphragm muscle. (A) Sections of diaphragm from experimental and control mice were stained with hematoxylin and eosin (H&E) and immunolabeled for minidystrophin (minidys) transgene expression detected with green fluorescence and stained with DAPI to detect nuclei (image bar = 200 μm). (B) Human minidystrophin-expressing muscle fibers were quantified and expressed as an average percentage of the total number of muscle fibers per section. Necrotic and regenerating muscle fibers were identified by binding to mouse immunoglobulin G (IgG) and expression of embryonic myosin heavy chain (eMyHC), respectively, and expressed as the average percentage of the total number of muscle fibers per section. Diaphragms from C57BL/10 healthy control mice lack human minidystrophin expression, necrosis and regeneration (data not shown in B). *Ex vivo* functional analysis of the diaphragm is shown by specific force production (N/cm²) (C) and as the percent force production in response to 10 isometric lengthening activations (D). All quantitative data are shown as mean ± standard error of the mean (SEM); *significant difference from untreated *mdx* mice ($P < 0.05$); n = number of animals analyzed. —◆—, C57BL/10; —✳—, untreated *mdx*; —□—, *mdx*, AAV + NBD peptide; —●—, *mdx*, AAV + saline.

RNA isolates before reverse transcription to cDNA, according to the manufacturer's instructions (Invitrogen). RNA/cDNA samples were analyzed using primers and dual-hybridization labeled probes for (a) the human minidystrophin construct in the AAV9 minidystrophin vector and (b) murine *GAPDH*, which is a reference gene that permits relative quantification of RNA data. qPCR reactions, set up in MicroAmp optical 96-well reaction plates (Applied Biosystems, Carlsbad, CA, USA), were performed in duplicate, in 50-μL volumes containing 10 μL of quadriceps genomic DNA or cDNA from reverse-transcribed RNA, 1 μL of 10 μmol/L forward and reverse primer, 2 μL of 5 μmol/L-labeled probe, 25 μL TaqMan 2× Universal Master Mix and 11 μL nuclease-free water (Applied Biosystems). Target sequences were amplified at the following conditions: 1 cycle of 50°C for 2 min and 95°C for 10 min, followed by 40 cycles of 95°C for 15 s and 60°C for 1 min, with fluorescent emissions captured using the Applied Biosystems 7300 Real-Time PCR System. Random PCRs were electrophoresed on a 1% agarose gel to ensure production of a single PCR product per primer/probe set. Primers and probe for the AAV9 minidystrophin construct were determined using Primer Express software (Applied Biosystems): AAV9 minidystrophin forward primer: 5′-GGACG GCAAC CACAA GCT-3′; AAV9 minidystrophin reverse primer: 5′-GTTTC TGGTG CTCTG CCTC-3′; AAV9 minidystrophin dual-hybridization probe: 5′-/56-FAM/TGGGC CTGAT CTGGA/36-TAMSp/-3′ (purchased from Integrated DNA Technologies, Coralville, IA, USA). Primers and probe design for the *ApoB* internal control for genomic DNA analysis were previously described (25). For a *GAPDH* internal control for RNA/cDNA real-time PCR analysis, we used the Mouse *GAPDH* Endogenous Control kit, using the VIC/MGB fluorescence/quencher motifs (Invitrogen).

Serum Analysis of α-Sarcomeric Actin

To assess whole mouse levels of muscle damage, we analyzed serum from ex-

quadriceps tissue using TRIzol Reagent (Invitrogen), according to the manufacturer's instructions. Isolated mRNA (1 μg) was reverse-transcribed to cDNA

using the SuperScript III First-Strand Synthesis System for RT-qPCR (real-time quantitative polymerase chain reaction) (Invitrogen), using DNase1 to pretreat

perimental and control mice for the presence of the intracellular muscle protein, α-sarcomeric actin, as previously described (26). Briefly, >95% purified, 43-kDa skeletal muscle actin protein (Cytoskeleton, Denver, CO, USA) was serially diluted to generate a standard curve to determine the µg/mL concentration of α-sarcomeric actin in serum of experimental and control mice. Mouse serum samples were diluted 1:5 in sterile 1× phosphate-buffered saline, pH 7.4, and then mixed with 5× Laemmli buffer (62.76 mmol/L Tris-HCl, pH 6.8, 10% glycerol, 1% SDS, 0.01% bromophenol blue and 1% β-mercaptoethanol) and heated at 94°C for 5 min. Samples were separated on a 10% denaturing polyacrylamide gel at 100 V for 2 h, and gels were transferred to nitrocellulose membranes at 100 V for 1 h. Blots were incubated with 1:200 diluted mouse–anti-α-sarcomeric actin antibody (Santa Cruz Biotechnology), followed by 1:5,000 diluted HRP-sheep anti-mouse IgG secondary antibody (Invitrogen). Blots were exposed to autoradiographic film for 2.5 min. All autoradiographic films were scanned, and densitometry was performed using ImageJ software.

Statistics

For statistical analysis between age-matched untreated *mdx* mice, AAV + NBD peptide–treated *mdx* mice and AAV + saline–treated *mdx* mice, one-way analysis of variance was used to determine statistical significance ($P < 0.05$). The number of animals used for each experiment is shown.

RESULTS

AAV9 Minidystrophin Gene Transfer to *mdx* Diaphragm Muscle

In diaphragm muscles from AAV + NBD peptide– and AAV + saline–treated *mdx* mice, 96% and 97% of muscle fibers, respectively, expressed minidystrophin localized to the sarcolemmal membrane 9 wks after neonatal intraperitoneal injection of AAV9 minidystrophin vector (Figures 1A, B). Significant reductions in
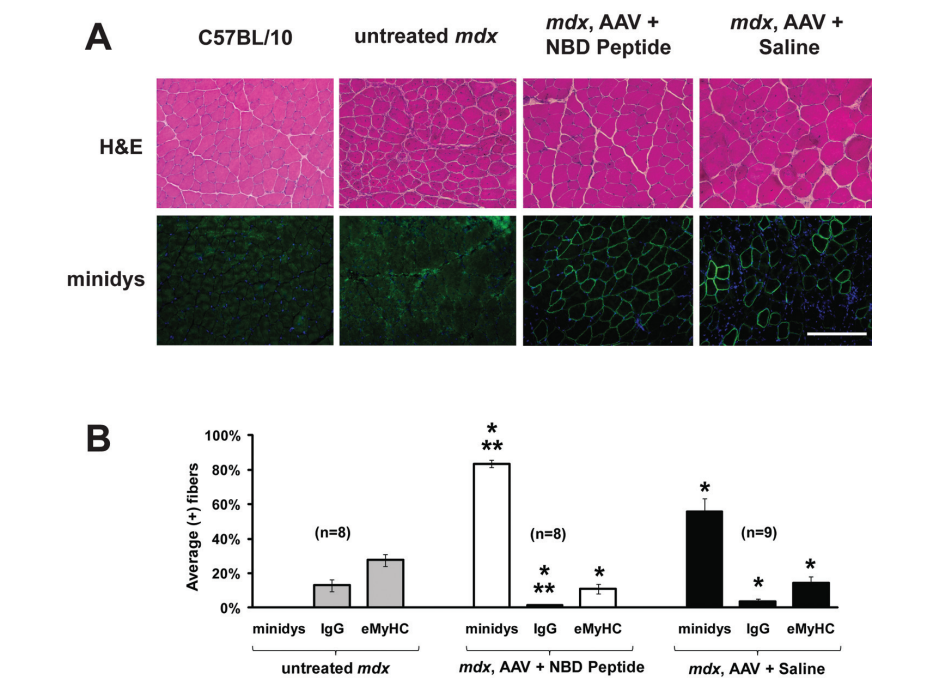

Figure 2. Morphology and human minidystrophin expression analysis of quadriceps muscle. (A) Sections of quadriceps muscle were studied with hematoxylin and eosin (H&E) staining and immunohistochemical detection of human minidystrophin expression (image bar = 200 µm). (B) Quantitative analysis of transgene expression (minidys), necrosis (IgG) and regeneration (eMyHC) is shown as the average percentage of positive fibers per total number of muscle fibers per section. Quadriceps from C57BL/10 healthy control mice lack human minidystrophin expression, necrosis and regeneration (data not shown in B). All quantitative data are shown as mean ± SEM; *significant difference from untreated *mdx* mice ($P < 0.05$); **significant difference from AAV + saline–treated *mdx* mice ($P < 0.05$); n = number of animals analyzed.

levels of necrosis ($P < 0.001$) and regeneration ($P < 0.001$) were observed in transduced diaphragms from both groups of experimental mice when compared with untreated *mdx* control animals (see Figure 1B). The high-level gene transduction of the diaphragm ameliorated the dystrophic phenotype, as shown by hematoxylin and eosin–stained sections, with normalization of fiber size, low incidence of centralized nuclei and an absence of immune cell infiltrate (see Figure 1A).

Functional Analysis of Costal Diaphragm from Experimental and Control Mice

At the time of sacrifice, multiple functional parameters of diaphragm muscles from experimental and control animals were analyzed. Specific force and the response to lengthening activations were

assayed to determine the ability of diaphragm muscle to function under physiological stress. Compared to untreated *mdx* mice, specific force production by diaphragm from the AAV + NBD peptide–treated ($P = 0.004$) and AAV + saline–treated ($P = 0.001$) *mdx* mice was significantly higher (Figure 1C). C57BL/10 healthy control mice exhibited the highest levels of specific force. Force production in response to a series of lengthening activations decreased 20.8% in untreated *mdx* mice. The AAV + NBD peptide– and AAV + saline–treated *mdx* mice yielded only a 9.3% ($P = 0.022$ compared with untreated *mdx*) and 9.9% ($P = 0.028$ compared with untreated *mdx*) loss in force production, respectively, after the 10 lengthening activations (Figure 1D). Furthermore, there was no significant
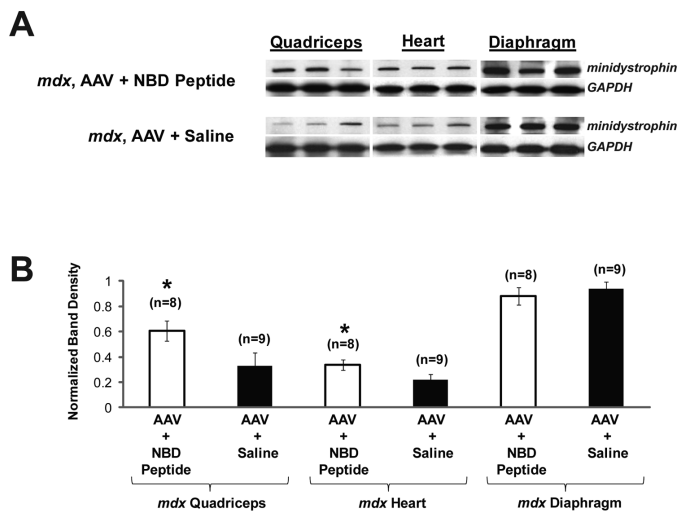
Figure 3. Quantification of human minidystrophin expression in quadriceps, heart and diaphragm muscles. Minidystrophin transgene protein expression was detected from total protein extracts by Western blot analysis. (A) Three representative bands reflecting the range of results are shown for quadriceps, heart and diaphragm muscles. There is no human minidystrophin expression in quadriceps, heart and diaphragm in *mdx* and C57BL/10 controls (data not shown). (B) Densitometric quantification of bands from all mice in each group was normalized to GAPDH expression. All quantitative data are shown as mean ± SEM.; *significant difference from AAV + saline–treated *mdx* mice (*P* < 0.05); n = number of animals analyzed.

difference in response to lengthening activations between C57BL/10 healthy control mouse diaphragm compared with diaphragm of *mdx* mice treated with AAV + NBD peptide (*P* = 0.493) or AAV + saline (*P* = 0.376).

AAV9 Minidystrophin Gene Transfer to *mdx* Quadriceps Muscle

We observed significantly higher minidystrophin expression in quadriceps muscle of AAV + NBD peptide–treated *mdx* mice (84% fibers expressed minidystrophin) as compared with the AAV + saline–treated *mdx* mice (56% fibers expressed minidystrophin, *P* = 0.000) (Figures 2A, B). Hematoxylin and eosin staining of quadriceps muscle sections revealed improved muscle histopathology in both treatment groups; however, the AAV + NBD peptide–treated *mdx* mice appeared qualitatively healthier than the AAV + saline–treated *mdx* mice (see Figure 2A). We detected significantly lower levels of necrotic muscle fibers in the quadriceps

sections of the AAV + NBD peptide–treated *mdx* mice (*P* = 0.000) and AAV + saline–treated *mdx* mice (*P* = 0.001) when compared with untreated *mdx* mice (*P* = 0.000). Necrosis levels were also significantly reduced in AAV + NBD peptide–treated compared with AAV + saline–treated *mdx* mice (*P* = 0.001). Levels of regeneration in the AAV + NBD peptide and AAV + saline groups were significantly lower than in untreated *mdx* mice (*P* = 0.000 for both treated groups compared with untreated *mdx*) (see Figure 2B).

Quantification of Minidystrophin Transgene Expression

To confirm our immunohistochemistry results, levels of minidystrophin expression were quantified by Western blot analysis. The highest level of minidystrophin expression was detected in the diaphragm muscles of AAV + NBD peptide–treated and AAV + saline–treated *mdx* mice, with no significant difference between the two treatment groups (Fig-

ures 3A, B). In contrast, pairwise comparison between the AAV + NBD peptide–treated and AAV + saline–treated *mdx* mice showed significantly higher levels of minidystrophin transgene expression in the quadriceps (*P* = 0.037) and cardiac tissue (*P* = 0.043) with the addition of NBD peptide–mediated therapy.

Reduction of NF-κB Activation After AAV Minidystrophin Gene Transfer and 8K-NBD Peptide Treatments

By electrophoretic mobility gel shift assay, we detected high levels of NF-κB protein in the nuclear extracts of age-matched diaphragm and quadriceps muscles from untreated *mdx* mice at 9 wks of age. Age-matched C57BL/10 mice exhibited a low basal level of NF-κB activation in both diaphragm and quadriceps (Figures 4A, B). In nuclear extracts from diaphragm and quadriceps from *mdx* mice treated with AAV + NBD peptide, we found significantly lower levels of NF-κB activation when compared with untreated *mdx* mice (*P* = 0.002 and 0.006, respectively) (see Figure 4B). In the AAV + saline–treated *mdx* mice, we observed a significant reduction in NF-κB activation in only the diaphragm muscle (*P* = 0.001), whereas reduction in the quadriceps did not reach significance (*P* = 0.167) (see Figure 4B).

Biodistribution of Minidystrophin Transgene Expression

The significantly different levels of minidystrophin transgene expression detected in the quadriceps of the AAV + NBD peptide–treated compared with the AAV + saline–treated *mdx* mice prompted us to determine levels of minidystrophin expression in other skeletal muscles and heart of the AAV + NBD peptide– and AAV + saline–treated *mdx* mice. Immunohistochemical analysis of gastrocnemius, tibialis anterior, triceps, heart and tongue muscle from representative mice from each group revealed higher levels of minidystrophin expression in all muscles and heart of the AAV +
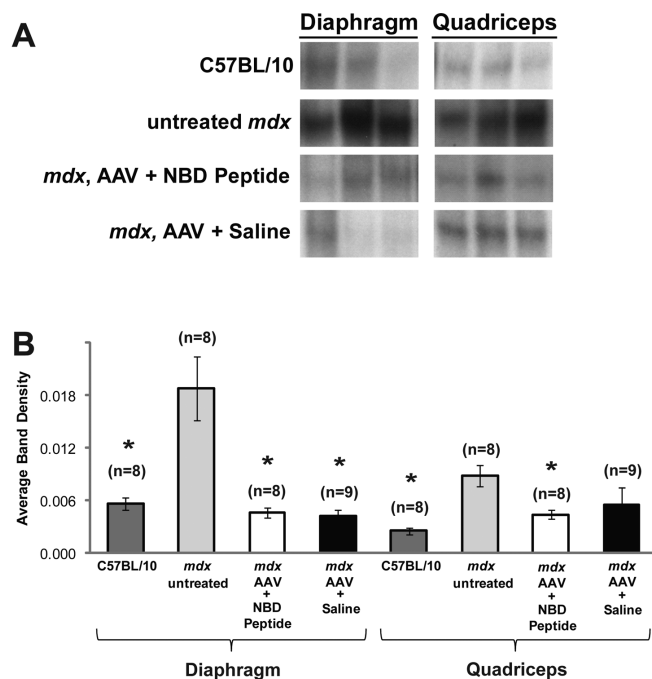
Figure 4. Activation of NF-κB. (A) NF-κB activation was analyzed by electrophoretic mobility shift assay of nuclear protein extracts of diaphragm and quadriceps muscle tissue in age-matched, untreated C57BL/10 and *mdx* mice and AAV + NBD peptide– and AAV + saline–treated *mdx* mice. Three representative bands reflecting the range of results are shown. (B) Densitometric quantification of bands from all treated and control mice were averaged and are presented as mean ± SEM. *Significant difference from untreated *mdx* mice (*P* < 0.05); n = number of animals analyzed.

NBD peptide–treated *mdx* mice, compared with AAV + saline–treated *mdx* mice (Figure 5). Thus, the initiation of 8K-NBD peptide treatments 26 d after neonatal gene transfer promoted expression of the minidystrophin vector to widespread muscles and heart in *mdx* mice.

Real-Time qPCR Analysis for Vector DNA and Vector mRNA Transcripts

Vector DNA copy number and mRNA transcripts from quadriceps muscles of AAV + NBD peptide– and AAV + saline–treated *mdx* mice were analyzed to elucidate a potential mechanism behind the higher levels of minidystrophin expression observed in the AAV + NBD peptide–treated *mdx* mice compared with AAV + saline–treated *mdx* mice in all muscles with the exception of diaphragm, where expression was near maximal in both groups. We detected nonsignificant differences of vector genome content be-

tween the two treated groups: 1.1 ± 0.21 vector genomes/nucleus in the AAV + NBD peptide group and 0.7 ± 0.30 vector genomes/nucleus in the AAV + saline group ($P = 0.301$) (Figure 6A). With similar levels of vector DNA in both treatment groups, we quantified vector mRNA transcripts after reverse transcription of RNA to cDNA. The AAV + NBD peptide–treated mice had a $2^{\delta\delta ct}$ relative value of $3.0e^{-8} \pm 5.4e^{-9}$, whereas the AAV + saline–treated mice had a significantly lower $2^{\delta\delta ct}$ relative value of $1.1e^{-8} \pm 5.0e^{-9}$ ($P = 0.023$) (Figure 6B).

Analysis of α-Sarcomeric Actin in Serum of Experimental and Control Mice

In the setting of muscle damage, contraction-induced injury or the degenerative dystrophic process, the intracellular sarcolemma-associated muscle protein α-sarcomeric actin is released to the
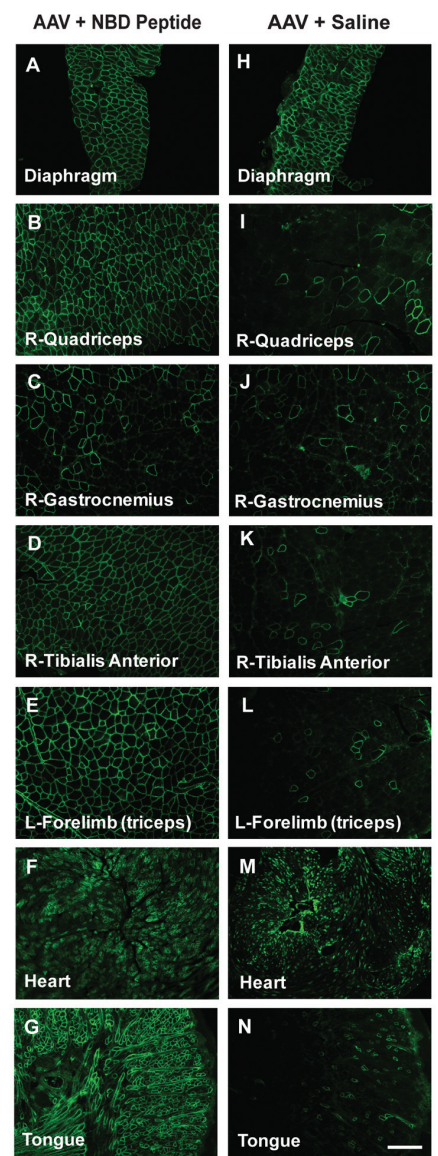

Figure 5. Biodistribution of minidystrophin transgene expression. Sections of muscle tissues (diaphragm, quadriceps, tibialis anterior, gastrocnemius, forelimb triceps, heart and tongue) were analyzed for human minidystrophin expression by immunohistochemistry to assess levels and distribution of transgene expression from the AAV minidystrophin vector with (AAV + NBD peptide) or without (AAV + saline) treatment with the 8K-NBD peptide. One representative mouse from each treatment group is shown. Representative images are from individual muscles of AAV + NBD peptide–treated (A–G) and AAV + saline–treated (H–N) groups. Image bar = 200 μm. L, Left; R, right.
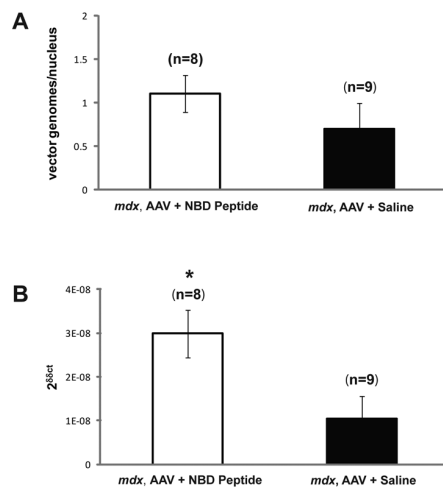
Figure 6. Quantification of vector DNA and mRNA transcripts in quadriceps. DNA and RNA were isolated from quadriceps muscle tissues from AAV + NBD peptide– and AAV + saline–treated *mdx* mice and analyzed by real-time qPCR. Vector DNA levels were quantified by primers/probes specific for AAV9 minidystrophin DNA, using isolated AAV9 minidystrophin vector DNA to generate a standard curve. The numbers of nuclei per sample were quantified by real-time qPCR using primers/probes specific for the *ApoB* gene. (A) Vector copy numbers were normalized to nuclei copy number to yield vector genomes/nucleus. Isolated muscle mRNA was reverse-transcribed, and cDNA samples were analyzed by real-time qPCR with primers/probe specific for minidystrophin cDNA to assess levels of vector mRNA and also with primers/probe specific for GAPDH. (B) Vector mRNA expression was normalized to GAPDH. Data are shown as mean ± SEM; *significant difference from AAV + saline–treated *mdx* mice (*P* < 0.05); n = number of animals analyzed.

systemic circulation and can be detected in serum. In C57BL/10 control mice, we did not detect any α-sarcomeric actin in serum samples (Figures 7A, B), which reflects negligible muscle damage in healthy mice. However, we detected a serum level of 84.9 ± 10.0 μg/mL α-sarcomeric actin in untreated *mdx* mice, reflecting the widespread dystrophic change in muscles of the *mdx* mouse. Additionally, we detected a
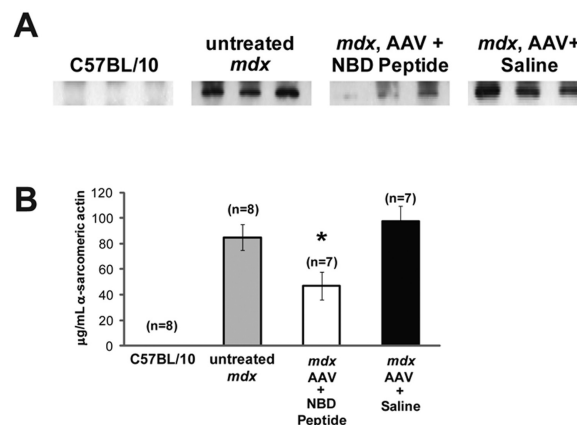
Figure 7. Muscle damage analysis. Serum from untreated C57BL/10, untreated *mdx*, AAV + NBD peptide–treated and AAV + saline–treated *mdx* mice was analyzed for the muscle protein α-sarcomeric actin, a marker of muscle degeneration. Serum levels (μg/mL) of α-sarcomeric actin were quantified using a standard curve of purified α-actin protein. (A) Representative bands from each of the treatment groups are shown. (B) Quantitative densitometry of samples from each control and treatment group is shown as mean ± SEM. *Significant difference from both untreated *mdx* and AAV + saline–treated *mdx* mice (*P* < 0.05); n = number of animals analyzed.

97.5 ± 11.7 μg/mL α-sarcomeric actin in the serum of the AAV + saline–treated *mdx* mice. In *mdx* mice treated with AAV + NBD peptide, we detected 46.9 ± 11 μg/mL α-sarcomeric actin in serum, marking a significant decrease in levels of α-sarcomeric actin in serum of these mice compared with untreated *mdx* mice (*P* = 0.019) and AAV + saline–treated *mdx* mice (*P* = 0.003) (see Figures 7A, B).

DISCUSSION

The high level of minidystrophin expression observed in diaphragm in both treatment groups of this study that were transduced with the AAV9 minidystrophin vector was associated with near total correction of morphological and functional abnormalities caused by dystrophy in *mdx* mice. The disease pathology of the *mdx* mouse diaphragm muscle is chronically progressive, similar to that observed in DMD patient muscle (27). Previous mouse gene transfer studies using AAV9 have shown reporter transgene expression in hindlimb, diaphragm and cardiac muscles of C57BL/10 mice (9), whereas studies using AAV9 vector in the *mdx* mouse disease model have largely focused on myocardium (28–30).

Data presented here adds to these studies by demonstrating the transduction efficiency and resultant therapeutic benefit of AAV9 minidystrophin gene transfer to the dystrophic diaphragm, limb muscle and myocardium. Because the usual cause of death in DMD patients is cardiac and respiratory failure, one result of our study, taken together with the prior published studies, emphasizes the potential role of AAV9 serotype-based gene therapy vectors for muscular dystrophy.

We and others have previously demonstrated the therapeutic benefits of NBD peptide treatment alone for *mdx* diaphragm and limb muscle (13,18,21). These previous NBD peptide studies showed reductions in muscle fiber necrosis and increases in muscle fiber regeneration in both diaphragm and hindlimb muscle. Furthermore, NBD peptide treatment resulted in significant increases in diaphragmatic muscle function in the *mdx* mouse. Levels of NF-κB activation were significantly reduced in NBD peptide–treated dystrophic mice. The current study extends the prior results by demonstrating that gene replacement therapy alone reduces the NF-κB activation level in muscle tissues that are highly trans-

duced by AAV9 minidystrophin compared with untreated mdx mice. Our previous studies demonstrated that treatment of mdx mice with NBD peptide alone reduced necrosis in the diaphragm by 40–55% (18). In the current study, we observed an almost 100% decrease in necrosis in the diaphragm of mice treated with AAV9 minidystrophin, with or without NBD peptide treatment. This result suggests that if gene replacement levels provide near-complete levels of transgene expression, then NBD peptide treatment does not improve on this short-term result, at least by the measured outcomes.

However, in the quadriceps muscle, we detected significantly higher levels of minidystrophin expression in the AAV + NBD peptide–treated mdx mice, which led to an 85% decrease in necrosis, compared with a 69% decrease in the AAV + saline–treated mdx mice. Therefore, treatment of mdx mice with the combination of NBD peptide and AAV9 minidystrophin gene transfer provided more robust therapy in limb muscle than AAV9 minidystrophin alone. In our previous study of NBD peptide treatment alone, we analyzed tibialis anterior muscle, which showed a 49–60% decrease in necrosis compared with mdx muscle. Although the limb muscle studied in the two studies differs, the result suggests that the addition of AAV9 minidystrophin gene transfer to NBD peptide treatment improved the therapeutic effect over NBD peptide treatment alone.

In addition to the above-mentioned results in quadriceps muscle and diaphragm, the present study demonstrates that the addition of NBD peptide therapy to AAV9 minidystrophin gene transfer results in widespread elevation of transgene expression throughout muscles of the hindlimb, forelimb, tongue and cardiac tissues compared with mdx mice treated with AAV9 minidystrophin gene transfer alone and leads to enhanced correction of dystrophic histopathology. This result was further explored by studying global muscle degeneration, as assessed by the detection

of α-sarcomeric actin levels in serum. Lower serum levels of α-sarcomeric actin were only observed with the combined treatment of AAV9 minidystrophin and NBD peptide. In contrast, despite high levels of minidystrophin transgene expression in diaphragm, the lower level of minidystrophin transgene expression in hindlimb and forelimb muscle observed with AAV9 minidystrophin gene transfer alone resulted in less of a reduction of serum levels of α-sarcomeric actin. It is likely that a threshold of minidystrophin expression must be achieved throughout muscles of the entire mouse to reduce serum α-sarcomeric actin, whereas strong, localized expression in only a small muscle such as the diaphragm may not be sufficient to reduce serum concentrations of α-sarcomeric actin. Thus, the combined therapeutic effects of NBD peptide plus AAV9 minidystrophin gene transfer offer the potential to promote successful therapeutic gene delivery to dystrophic tissue, leading to decreased degeneration of widespread muscle tissue.

In addition to differences in skeletal muscle, cardiac transduction was significantly higher in the AAV + NBD peptide–treated mdx mice, and this is a critical result, since a significant number of human DMD patients succumb to cardiac failure. Many previous studies have documented significantly reduced cardiac contractile performance by electrocardiogram in as early as 8-wk-old mdx mice (29), in trabeculae isolated from 8-wk-old mdx mice (31), in right ventricular trabeculae from 10-wk-old mdx mice (32) and in atria from 12- and 14-wk-old mdx mice (33). We did not perform cardiac muscle function in this current study, but can infer the potential effects of the high-level minidystrophin expression we observed in the myocardium on the basis of previous AAV-mediated mini- and microdystrophin gene delivery studies. In mdx mice treated systemically with an AAV2/6 microdystrophin vector, extensive gene transduction of cardiac tissue was observed, leading to a correction of baseline–end diastolic volume defect as

well as prevention of cardiac-pump failure induced by dobutamine (34). In another study, neonatal mdx mice were treated with an AAV–microdystrophin vector, and the heart was analyzed for uptake of Evans blue dye after a mechanical challenge to the heart in the form of β-isoproterenol injection (30). High-level microdystrophin expression provided protection of the myocardium as microdystrophin–positive fibers were all negative for EBD uptake (30). A third study used electrocardiograph analysis of C57BL/10, mdx and AAV9 minidystrophin–treated mdx mice to demonstrate improved cardiac performance 17–18 wks after neonatal AAV vector–treated mdx mice (28). High-level gene transfer to the myocardium was observed, which normalized multiple parameters related to cardiomyopathy, such as heart rate, PR interval and QT interval (28). Similarly, another group performed AAV9-mediated treatment of 4-wk-old mdx and analyzed mice 24 and 72 wks after injection, again revealing improvement in cardiac muscle function in response to vector administration (29). In our study, we observed similarly high levels of minidystrophin expression and would expect to see improvement in cardiac performance in vector-treated animals. However, further studies examining the role of NF-κB in the myocardium would be beneficial to determine if the NBD peptide addition to AAV9-mediated minidystrophin gene transfer could further improve cardiac performance in mdx mice.

The higher levels of transgene expression in mdx mice that were treated with both AAV9 minidystrophin gene transfer and NBD peptide therapy suggest that NBD peptide treatment may create a microenvironment in muscle conducive to strong, uninterrupted expression of the AAV9-delivered minidystrophin. The protection from dystrophic degeneration of mdx muscle treated with the combined therapy is an expected effect of high-level transgene expression that would limit cycles of degeneration and regeneration of vector-transduced, NBD peptide–treated muscle fibers. In contrast,

muscles of *mdx* mice treated with AAV9 minidystrophin gene transfer alone have lower levels of transgene expression that may allow a persistent inflammatory response in dystrophic tissue that could further limit minidystrophin transgene expression.

To explore why transgene expression in muscle was higher in most muscle tissues of *mdx* mice treated with combined therapy, we first examined vector genome content in quadriceps muscle to determine whether the addition of NBD peptide therapy to AAV9 minidystrophin gene therapy affected vector delivery or retention. Vector genome analysis demonstrated similar levels of vector DNA in quadriceps of both treatment groups, which suggested equal delivery and vector DNA retention in the muscle.

We next performed vector transcript analysis and demonstrated a significantly lower dystrophin mRNA expression level in *mdx* mice treated with AAV9 minidystrophin gene transfer alone, which suggested that the microenvironment in muscle fibers treated with NBD peptide may promote transcription from the CMV promoter that drives minidystrophin expression from the AAV9 vector. Interestingly, a previous study showed decreased expression from many viral promoters, including CMV, leading to attenuation of transgene expression from adenoviral, retroviral and plasmid vectors *in vitro*, in the presence of TNFα (35). In this previous study, TNFα did not affect vector DNA levels, but did affect transgene expression at the mRNA level, as shown by Northern blot analysis (35). These studies using other vector systems suggest an explanation for our observation of lower levels of mRNA transcripts despite equal amounts of vector DNA content in the *mdx* mice treated with AAV9 minidystrophin gene transfer alone. Taken together, these results plus the previously demonstrated increase in TNFα in muscles of *mdx* mice (16,36) suggest that *mdx* mice treated with AAV9 minidystrophin gene transfer and NBD peptide therapy likely had lower levels of circulating and muscle tissue TNFα that

thus promoted higher levels of transgene expression from the CMV promoter.

CONCLUSION

In summary, treatment of *mdx* mice with either NBD peptide or AAV9 minidystrophin gene transfer alone can reduce muscle necrosis and improve muscle function. However, the combination of AAV9 minidystrophin gene transfer with NBD peptide therapy shows the most significant improvement in the dystrophic *mdx* mouse, mainly due to the effect of the NBD peptide therapy on transgene expression provided by AAV9-mediated minidystrophin gene transfer. NBD peptide treatment may delay the progression of muscular dystrophy by multiple mechanisms, including a direct effect on dystrophic muscle, as we and others have previously shown (13,18,21), and by promotion of optimal viral vector-mediated gene delivery and expression. For example, NBD peptide adjunct therapy to AAV9 minidystrophin gene delivery may potentially lead to treatment with therapeutic vectors at lower doses, thus providing safer gene delivery. In future studies, it will be important to perform studies that combine AAV9 minidystrophin gene transfer using tissue-specific promoters with modalities to inhibit NF-κB activation.

ACKNOWLEDGMENTS

DISCLOSURE

The authors declare that they have no competing interests as defined by *Molecular Medicine*, or other interests that might be perceived to influence the results and discussion reported in this paper.

REFERENCES

1. Emery AE. (1991) Population frequencies of inherited neuromuscular diseases: a world survey. *Neuromuscul. Disord*. 1:19–29.
2. Emery AEH, Muntoni F. (2003) *Duchenne Muscular Dystrophy*. 3rd edition. Oxford; New York: Oxford University Press. 270 pp.
3. Ervasti JM, Campbell KP. (1993) Dystrophin-associated glycoproteins: their possible roles in the pathogenesis of Duchenne muscular dystrophy. *Mol. Cell. Biol. Hum. Dis. Ser*. 3:139–66.
4. Hoffman E, Brown R, Kunkel L. (1987) Dystophin: the protein product of the Duchenne Muscular Dystrophy locus. *Cell*. 51:919–28.
5. Zubrzycka-Gaarn EE, *et al.* (1988) The Duchenne muscular dystrophy gene product is localized in sarcolemma of human skeletal muscle. *Nature*. 333:466–9.
6. Bulfield G, Siller WG, Wight PA, Moore KJ. (1984) X chromosome-linked muscular dystrophy (mdx) in the mouse. *Proc. Natl. Acad. Sci. U. S. A*. 81:1189–92.
7. Wang B, Li J, Xiao X. (2000) Adeno-associated virus vector carrying human minidystrophin genes effectively ameliorates muscular dystrophy in mdx mouse model. *Proc. Natl. Acad. Sci. U. S. A*. 97:13714–9.
8. Watchko J, *et al.* (2002) Adeno-associated virus vector-mediated minidystrophin gene therapy improves dystrophic muscle contractile function in mdx mice. *Hum. Gene Ther*. 13:1451–60.
9. Inagaki K, *et al.* (2006) Robust systemic transduction with AAV9 vectors in mice: efficient global cardiac gene transfer superior to that of AAV8. *Mol. Ther*. 14:45–53.
10. Zincarelli C, Soltys S, Rengo G, Rabinowitz JE. (2008) Analysis of AAV serotypes 1–9 mediated gene expression and tropism in mice after systemic injection. *Mol. Ther*. 16:1073–80.
11. Eghtesad S, Zheng H, Nakai H, Epperly MW, Clemens PR. (2010) Effects of irradiating adult mdx mice before full-length dystrophin cDNA transfer on host anti-dystrophin immunity. *Gene Ther*. 17:1181–90.
12. Zaiss AK, Muruve DA. (2008) Immunity to adeno-associated virus vectors in animals and humans: a continued challenge. *Gene Ther*. 15:808–16.
13. Acharyya S, *et al.* (2007) Interplay of IKK/NF-kappaB signaling in macrophages and myofibers promotes muscle degeneration in Duchenne muscular dystrophy. *J. Clin. Invest*. 117:889–901.
14. Kumar A, Boriek AM. (2003) Mechanical stress activates the nuclear factor-kappaB pathway in skeletal muscle fibers: a possible role in Duchenne muscular dystrophy. *FASEB J*. 17:386–96.
15. Messina S, *et al.* (2006) Lipid peroxidation inhibition blunts nuclear factor-kappaB activation, reduces skeletal muscle degeneration, and enhances muscle function in mdx mice. *Am. J. Pathol*. 168:918–26.
16. Messina S, *et al.* (2006) Nuclear factor kappa-B blockade reduces skeletal muscle degeneration

and enhances muscle function in Mdx mice. *Exp. Neurol.* 198:234–41.

17. Monici MC, Aguennouz M, Mazzeo A, Messina C, Vita G. (2003) Activation of nuclear factor-kappaB in inflammatory myopathies and Duchenne muscular dystrophy. *Neurology.* 60:993–7.

18. Reay DP, *et al.* (2011) Systemic delivery of NEMO binding domain/IKKgamma inhibitory peptide to young mdx mice improves dystrophic skeletal muscle histopathology. *Neurobiol. Dis.* 43:598–608.

19. Tang Y, *et al.* (2010) Inhibition of the IKK/NF-kappaB pathway by AAV gene transfer improves muscle regeneration in older mdx mice. *Gene Ther.* 17:1476–83.

20. Rothwarf DM, Karin M. (1999) The NF-kappa B activation pathway: a paradigm in information transfer from membrane to nucleus. *Sci. STKE.* 1999:RE1.

21. Peterson JM, *et al.* (2011) Peptide-based inhibition of NF-kappaB rescues diaphragm muscle contractile dysfunction in a murine model of Duchenne muscular dystrophy. *Mol. Med.* 17:508–15.

22. Tilstra J, *et al.* (2007) Protein transduction: identification, characterization and optimization. *Biochem. Soc. Trans.* 35:811–5.

23. Kornegay JN, *et al.* (2010) Widespread muscle expression of an AAV9 human mini-dystrophin vector after intravenous injection in neonatal dystrophin-deficient dogs. *Mol. Ther.* 18:1501–8.

24. Watchko JF, Johnson BD, Gosselin LE, Prakash YS, Sieck GC. (1994) Age-related differences in diaphragm muscle injury after lengthening activations. *J. Appl. Physiol.* 77:2125–33.

25. Pan D, *et al.* (2002) Biodistribution and toxicity studies of VSVG-pseudotyped lentiviral vector after intravenous administration in mice with the observation of in vivo transduction of bone marrow. *Mol. Ther.* 6:19–29.

26. Martinez-Amat A, *et al.* (2005) Release of alpha-actin into serum after skeletal muscle damage. *Br. J. Sports Med.* 39:830–4.

27. Stedman HH, *et al.* (1991) The mdx mouse diaphragm reproduces the degenerative changes of Duchenne muscular dystrophy. *Nature.* 352:536–9.

28. Bostick B, *et al.* (2008) Adeno-associated virus serotype-9 microdystrophin gene therapy ameliorates electrocardiographic abnormalities in mdx mice. *Hum. Gene Ther.* 19:851–6.

29. Shin JH, *et al.* (2011) Improvement of cardiac fibrosis in dystrophic mice by rAAV9-mediated microdystrophin transduction. *Gene Ther.* 18:910–9.

30. Yue Y, *et al.* (2003) Microdystrophin gene therapy of cardiomyopathy restores dystrophin-glycoprotein complex and improves sarcolemma integrity in the mdx mouse heart. *Circulation.* 108:1626–32.

31. Janssen PM, Hiranandani N, Mays TA, Rafael-Fortney JA. (2005) Utrophin deficiency worsens cardiac contractile dysfunction present in dystrophin-deficient mdx mice. *Am. J. Physiol. Heart Circ. Physiol.* 289:H2373–8.

32. Xu Y, Delfin DA, Rafael-Fortney JA, Janssen PM. (2011) Lengthening-contractions in isolated myocardium impact force development and worsen cardiac contractile function in the mdx mouse model of muscular dystrophy. *J. Appl. Physiol.* 110:512–9.

33. Sapp JL, Bobet J, Howlett SE. (1996) Contractile properties of myocardium are altered in dystrophin-deficient mdx mice. *J. Neurol. Sci.* 142:17–24.

34. Townsend D, *et al.* (2007) Systemic administration of micro-dystrophin restores cardiac geometry and prevents dobutamine-induced cardiac pump failure. *Mol. Ther.* 15:1086–92.

35. Qin L, *et al.* (1997) Promoter attenuation in gene therapy: interferon-gamma and tumor necrosis factor-alpha inhibit transgene expression. *Hum. Gene Ther.* 8:2019–29.

36. Machado RV, *et al.* (2011) Eicosapentaenoic acid decreases TNF-alpha and protects dystrophic muscles of mdx mice from degeneration. *J. Neuroimmunol.* 232:145–50.